Spatially limited ion acoustic wave activity in low-pressure helicon discharges

C. S. Corr, N. Plihon, and P. Chabert
Laboratoire de Physique et Technologie des Plasmas, Ecole Polytechnique, Palaiseau 91128, France

O. Sutherland and R. W. Boswell
Plasma Research Laboratory, School of Physical Science and Engineering, Australian National University, Canberra, Australia

(Received 7 April 2004; accepted 1 July 2004; published online 8 September 2004)

Ion acoustic wave phenomena are studied and compared in two low-pressure argon discharges created by helicon sources. The wave amplitudes are spatially localized near the edge of a plasma column as the amplitudes of the "mirror waves" that are separated from the helicon source frequency by the ion wave frequency. Dependencies of the ion wave on radial position, pressure, input power, and magnetic field are investigated. Measurements of the wavelength show that the wave is traveling azimuthally at approximately the ion sound speed in the direction of electron gyration. Although the wave spectra are indicative of a parametric decay phenomenon, it seems more likely that the radial plasma pressure gradient drives an ion acoustic instability which then modulates the helicon source. © *2004 American Institute of Physics*. [DOI: 10.1063/1.1785790]

I. INTRODUCTION

Helicon plasma sources[1] have generated much interest in the plasma processing community due to their ability to produce high etch rates and high selectivity.[2] They are being studied not only for use in industrial applications such as plasma processing of semiconductors and space plasma thrusters, but also for the understanding of basic plasma physics processes.[3–5] Helicon (or whistler) waves are a simplified form of right hand polarized electromagnetic waves in a magnetized plasma with frequencies between the lower-hybrid and electron cyclotron frequencies. The coupling of rf power to a helicon discharge can occur in three modes. At low input power the discharge is ignited in a low density (10^9 cm^{-3}) capacitive (E) mode. At a higher input power there is a transition to a higher density (10^{10} cm^{-3}) inductive (H) mode. By further increasing the input power a transition occurs to a high density ($>10^{11}$ cm^{-3}) helicon wave (W) mode.

This study is motivated by an interest in plasma diffusion across magnetic fields, instabilities, and a general understanding of plasma processes both in electropositive and electronegative gases. Plasma flow across magnetic fields may give rise to a large number of instability mechanisms.

Parametric decay of whistler waves has been known for many decades with the first experimental evidence observed in a strongly magnetized plasma cylinder[6] operated with a powerful pump wave of 2.45 GHz and up to 6 kW input power. Plasma densities of up to 10^{13} cm^{-3} were created. The pump wave decayed into another whistler wave and a short wavelength ion acoustic wave at around 7 MHz. The authors remarked that significant heating of about 10% of both the ions and electrons accompanied the parametric decay for a pump frequency of about $0.7f_{ce}$.

Boswell and Giles[7] operating in a large area plasma at 0.5 mTorr with an applied axial magnetic field of 128 G, and a measured electron density of 6×10^{10} cm^{-3}, observed decay waves that were only seen along the group velocity resonance cones. Pump waves at 150 MHz ($0.42f_{ce}$) were transmitted from a 1 cm diameter loop antenna and received with a small floating Langmuir probe. The low-frequency ion waves had a frequency of 150 kHz, and were only seen above a threshold power and at 28° to the magnetic field and not elsewhere.

More recently, Kline *et al.*[8,9] have presented experimental evidence in a helicon source of the parametric decay of the helicon wave at a frequency around 10 MHz into two electrostatic waves, thought to be a lower hybrid wave and an ion acoustic wave. They observed a maximum amplitude of the parametrically excited wave that could be as large as 8% of the pump wave. The wave was localized near the axis of the helicon source for radii less than 3 cm. Frequencies in the range 400–800 kHz were observed.

Virko *et al.*[10] operating in a 1 mTorr argon discharge driven at 13.56 MHz observed oscillations in the frequency range about 1 MHz that the authors say were due to the interaction of the rf field with the plasma. The excitation of these low-frequency oscillations had thresholds in input power and dc magnetic field suggesting that parametric decay was the likely phenomenon.

One of the problems in analyzing these low-frequency ion waves is finding the energy source that drives the wave. In the papers cited above, the waves with frequencies of hundreds of kilohertzs are generally considered to be a result of a three wave parametric decay with the helicon wave being the pump wave. If the decay originated from the electromagnetic fields of the helicon wave, it would be reasonable to find the decay waves having maximum amplitude in or near the center of the discharge where the helicon electric fields are maximum. However, if the electrostatic resonance cone fields, or possibly the near fields of the antenna itself, drove the decay, the decay products would be expected to be

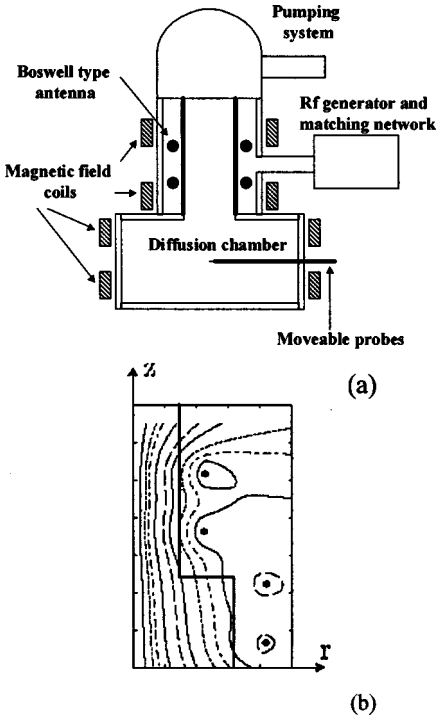

FIG. 1. Schematic diagram of (a) the helicon plasma source and (b) the corresponding calculated magnetic field lines.

maximum near the plasma boundaries. Unfortunately, near the plasma boundaries, there are commonly severe gradients in plasma density and electron temperature which are not an inconsiderable source of free energy. The effect of gradients as an energy source for low-frequency ion instabilities has been investigated by many authors and recently by Light *et al.*[11] for a helicon discharge. They measure low-frequency waves around 10 kHz (ten times lower than measured here) and developed a theory based on azimuthal drift driven by pressure gradients.

In this paper we present experimental measurements of low-frequency ion acoustic wave phenomena in helicon plasma sources operated at Ecole Polytechnique, Palaiseau (E.P.) and in WOMBAT (waves on magnetized beams and turbulence) operated at the Australian National University, Canberra. The major difference between the two systems is that WOMBAT has four times the volume. In Sec. II the helicon sources and the experimental diagnostics are described. Experimental results obtained in the two sources are presented in Sec. III. Section IV discusses and draws some conclusions to this experimental work.

II. EXPERIMENTAL APPARATUS AND DIAGNOSTICS

A. Ecole Polytechnique

A schematic diagram of the helicon plasma source and the calculated magnetic field lines used in all experiments at E.P. are shown in Fig. 1. The reactor consists of a source and a diffusion chamber [Fig. 1(a)]. The source is a 14 cm diameter, 30 cm long, and 0.7 cm thick pyrex cylinder surrounded by a double saddle field type helicon antenna.[12] The fan-cooled antenna is powered through a close-coupled *L*-type matching network by a rf power supply operating at 13.56 MHz and capable of delivering 2 kW forward power. The input power was recorded as the difference between the forward and reflected powers. The pyrex cylinder is housed in an aluminum cylinder of 20 cm diameter and 30 cm long surrounded by two magnetic field coils and sits atop a 32 cm diameter, 24 cm long diffusion chamber also surrounded by two field coils. The currents in the coils were such that the most uniform magnetic field for this configuration was obtained [Fig. 1(b)]. Visually the plasma is observed to be cylindrical in the diffusion chamber directly under the source region. The magnetic field is maximum along the axis ($r=0$) in the diffusion chamber of the reactor with a value of 34 G. A turbomolecular pump attached to the other end of the source tube routinely achieves base pressures of 10^{-6} mbar.

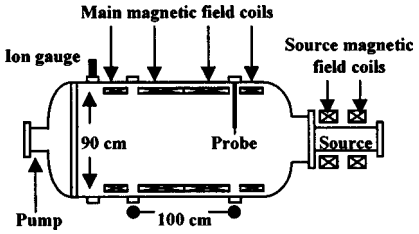

FIG. 2. Schematic diagram of WOMBAT.

All measurements reported here were made in the diffusion chamber 12 cm from the source/diffusion interface, i.e., in the median plane of the diffusion chamber. Probes attached to a translating system were inserted radially into the diffusion chamber [Fig. 1(a)] for spatially resolved measurements. A passively compensated Langmuir probe,[13] of 0.25 mm diameter and 5 mm long tungsten wire tip, was used to find the plasma parameters from measurements of the probe $I(V)$ characteristics using a Smartsoft data acquisition system.[14] An uncompensated unbiased Langmuir probe was connected to a spectrum analyzer via a dc block and used to measure the wave spectra. The ion wave velocity was determined by measuring the phase shift between the signals detected by two unbiased, uncompensated probes with the probe tips positioned at $r=7$ cm and separated by a distance of 4.5 mm.

B. Australian National University

The large plasma diffusion system used in Canberra, WOMBAT,[15] has been described elsewhere but it briefly consists of a glass source tube 50 cm long and 18 cm in diameter attached on axis to a large stainless steel diffusion chamber 200 cm long and 90 cm inner diameter, as shown in Fig. 2. A grounded aluminium plate terminates the other end of the source. A steady axial magnetic field is maintained by a set of external solenoids surrounding the source and a large solenoid inside the diffusion chamber. In these experiments, the source solenoids were not used. As a result the magnetic field was highly uniform inside the diffusion chamber but divergent in the source. The exact geometry of the magnetic field outside the diffusion chamber has not been measured. A base pressure of 4×10^{-6} Torr is maintained in the vacuum

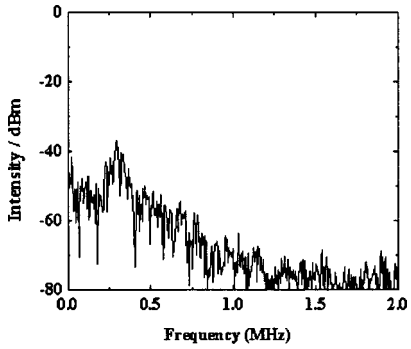

FIG. 3. The broadband wave spectra observed at 3 mTorr and 200 W.

chamber by a turbomolecular pump attached to the chamber end opposite the source. Operating pressures of 0.5–3 mTorr are set using a mass flow controller and an ion gauge. A rf power supply provides up to 2.5 kW of forward power at a frequency of 7.2 MHz to a double half-turn antenna via a π-matching network. The antenna is 20 cm in diameter, 1 cm wide, and 0.3 cm thick and is positioned around the outside of the glass source tube, directly below the matching box and 7.5 cm from the aluminium end plate. The top of the antenna is connected to the matching box and the bottom to a grounded cylindrical aluminium electric shield situated between the source tube and the source solenoids.

A noncompensated, translating Langmuir probe was inserted radially into the diffusion chamber 100 cm from the source end plate. The probe consisted of two nickel wires 250 μm in diameter and 4 mm long, electrically isolated from each other and shielded by a 6 mm diameter earthed steel tubing the whole extent of the probe length up to the probe tips. The 200 mm preceding the probe tips was coated with high temperature ceramic. The remainder of the probe consisted of a grounded steel tube. This probe construction was originally intended for spectral cross-correlation measurements but in these experiments was simply used as an individually floating Langmuir probe. Moreover, the upstream probe tip (that which was closest to the source with the plane of the probe tips parallel to the axis of the device) was used for the measurements presented in this paper. The radial translation of the probe was set using a computer controlled stepper motor arrangement that allowed the probe tip position to be selected with an accuracy of a few micrometers. Wave spectra were obtained by digitizing (12 bit) the analog output of a heterodyne spectrum analyzer connected to the floating probe via a dc block.

III. RESULTS

A. Wave spectra

In both systems, the low-frequency waves are characterized by a broadband structure that extends out to about 1 MHz. At E.P. there is a broad maximum for frequencies below around 300 kHz as can be seen in Fig. 3 and in WOMBAT the maximum occurs for about half of that frequency. Depending on conditions of pressure, rf power, and matchbox tuning, very narrow peaks are observed in both

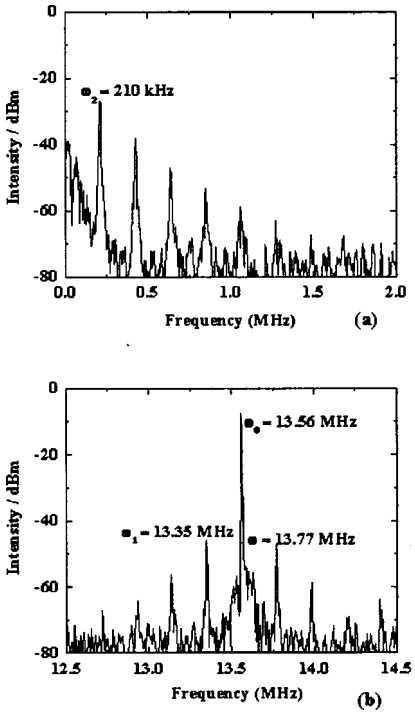

FIG. 4. The frequency spectrum obtained at E.P. showing (a) the low-frequency wave and (b) the upper and lower sideband peaks which are displaced from the rf pump frequency (13.56 MHz) by its frequency. Experimental conditions are 3 mTorr and 400 W.

systems, the maximum amplitude of the fundamental generally corresponding to the maximum in the broadband noise.

An example of the narrow peaks measured at E.P. is shown in Fig. 4(a) at a gas pressure of 3 mTorr and 400 W input power. A low-frequency wave can be seen at 210 kHz and a number of harmonics can also be observed at higher frequencies with lower amplitudes [Fig. 4(a)]. These higher frequency harmonics depend sensitively on the operating conditions and at times only the low-frequency wave is observed. Mirror waves are observed on either side of the pump wave (13.56 MHz) that are displaced by exactly the frequency of the low-frequency wave [Fig. 4(b)]. Depending on the operating conditions, the signal strength of the upper sideband wave may be either larger or smaller than the lower sideband wave. The relative amplitudes shown in the wave spectra of Figs. 3 and 4 were obtained using a digital oscilloscope fast Fourier transform (FFT) and can be regarded as only approximate.

In WOMBAT a number of clear peaks are discerned at different frequencies in the spectrum, however, the strongest intensity waves are detected in the 100 kHz range [Fig. 5(a)]. The nature of the two smaller waves 10 kHz above and below the 100 kHz wave have not been determined. The 100 kHz waves exist over the broadest range of parameters and were detected consistently during every run. The parameter range used to study these 100 kHz waves in WOMBAT were 0.5–3 mTorr in pressure (higher pressures were not investigated as the narrow peaks disappeared at 3 mTorr, although the broadband structure remained), 50–2500 W in forward power, and 50–170 G in magnetic field. As shown in Fig. 5(b), the low-frequency 100 kHz wave is mirrored by

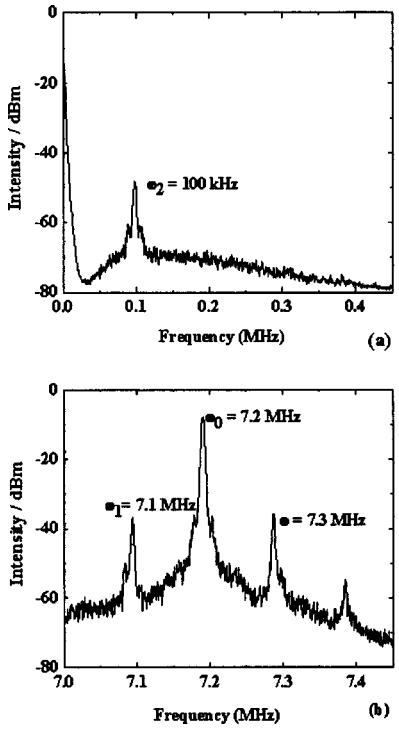

FIG. 5. (a) The 100 kHz wave can be clearly discerned 20 dB above the broadband structures. (b) The "mirror" waves can be seen 100 kHz on either side of the pump wave 25 dB above the broadband structures.

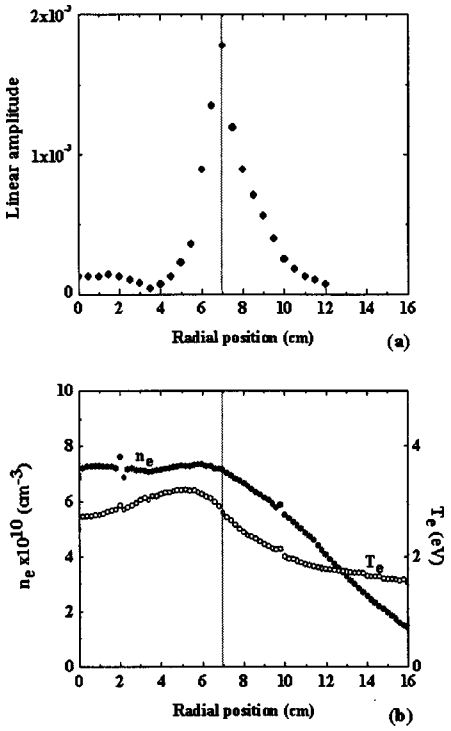

FIG. 6. The radial dependence of (a) the ion acoustic wave amplitude and (b) the electron density (closed circles) and electron temperature (open circles) at 3 mTorr and 400 W in the E.P. system.

two other waves 100 kHz above and below the pump wave (7.2 MHz). The nature of the signal 200 kHz above the pump has not been investigated.

B. Localization

The low-frequency waves are spatially localized away from the center for all experimental conditions of power and pressure in the two reactors. Figure 6(a) shows the radial dependence of the low-frequency wave amplitude at a pressure of 3 mTorr and an input power of 400 W obtained at E.P. In the figure $r=0$ cm is the diffusion chamber center and $r=16$ cm is the diffusion chamber wall. The line at $r=7$ cm corresponds to the edge of the source chamber (and the edge of the plasma column in the diffusion chamber). The low-frequency wave is strongest at the edge of the plasma column, i.e., 7 cm.

Interestingly, the location of maximum amplitude of the wave corresponds to the start of strong gradients in the plasma parameters. Figure 6(b) shows the radial profile of the electron density and temperature measured in the E.P. helicon plasma source at 400 W for a gas pressure of 3 mTorr. Both of these parameters are reasonably constant to the radius of the source at 7 cm and then both decrease towards the chamber wall at $r=16$ cm. Hence there is a gradient in the plasma pressure that would be an important source of free energy in this system.

In WOMBAT, the 100 kHz wave is also found in the outer layer of the plasma column [Fig. 7(a)], for all pressures investigated, where again there are strong gradients in the plasma pressure. Figure 7(b) presents the electron density and electron temperature as a function of radial position and a very sharp gradient is observed at the edge of the column between 2 and 10 cm. The line at $r=9$ cm corresponds to the edge of the source chamber. With the magnetic field configuration employed here very high densities can be achieved in WOMBAT, and the present results were taken in the high density "blue mode" which is characterized by extremely strong emissions from ArII lines and very little from ArI, implying that the central plasma is highly ionized with very few neutrals present.

Comparing with Fig. 6(a), it is clear that the peak in the 100 kHz signal intensity occurs at the mid-point of the high gradient region (~6 cm). Interestingly there is a small region away from the column, between 12 and 14 cm, where well-defined peaks are also observed, though it is noted that the signal strength (as well as the signal to noise ratio) is orders of magnitude lower (on some runs these peaks were not discernable). Elsewhere in the plasma the 100 kHz wave is indistinguishable from the surrounding broadband structure and is at least 40 dB lower than the maximum.

We repeat that the broadband low-frequency noise in the E.P. system extends to 1 MHz and in WOMBAT to 450 kHz with the narrow band waves being observed at the maximum of the broadband noise. Both the broadband and narrow band low frequencies have the same radial structure with a clear maximum at the edge of the plasma and not in the center as observed by other researchers.[8–10]

C. Wave velocity

The velocity of the wave has been investigated in the E.P. reactor using two unbiased uncompensated Langmuir probes with tips separated by a distance of 4.5 mm (x) in the

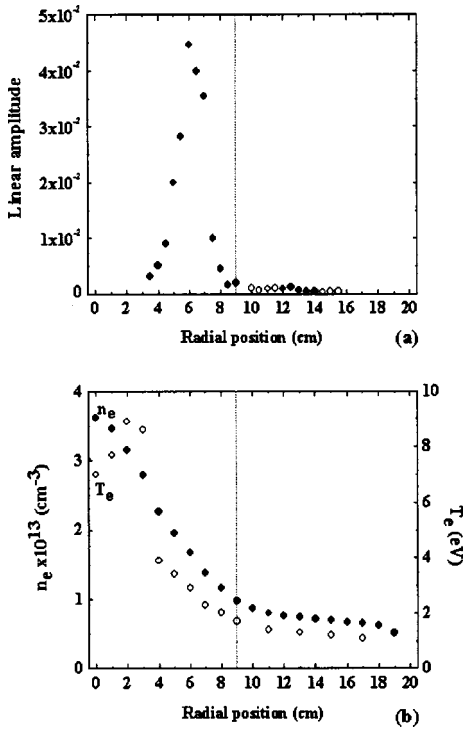

FIG. 7. (a) The 100 kHz signal amplitude as a function of position. The closed circles represent well defined peaks and the open circles represent the the broadband signal. (b) The electron density (closed circles) and electron temperature (open circles) as a function of radial position for a magnetic field of 150 G, 1.2 mTorr, and 2000 W.

median plane of the diffusion chamber. The two probes have the same axial position, which leads to the measurement of the azimuthal velocity of the 210 kHz wave. The velocity was obtained by computing the cross-correlation spectrum of the time varying floating potential signals from the two probes. The phase difference $\Delta\varphi$ between the two signals for the wave is obtained as the cross-correlation spectrum phase at 210 kHz and the velocity is calculated from $v=\omega x/\Delta\varphi$. From this analysis the wavelength of the low-frequency wave is calculated to be $\approx$1 cm that corresponds to a velocity of the order of the ion sound speed and, as can be seen in Fig. 8, this statement holds true for a broad range of pressure. This leads to conclude that the wave described in this study is an ion acoustic wave that propagates in the direction given by the product of the $-\mathrm{grad}(n_c)\times B$, i.e., the direction of the electron gyration.

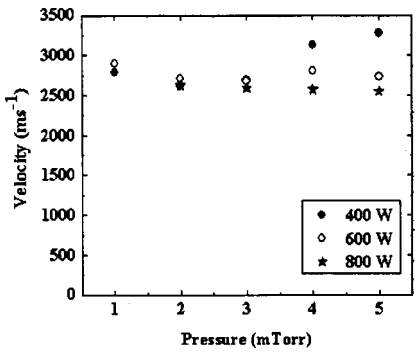

FIG. 8. The velocity of the ion acoustic wave vs pressure measured in the E.P. system.

D. Pressure

At E.P. the frequency of the ion wave is found to be weakly dependent on gas pressure and increase by less than a factor of 2 for a pressure change from 1 to 10 mTorr with increasing pressure. The wave amplitude decreases when the pressure is increased perhaps caused by the increase in collisional damping. Below 0.3 mTorr the low-frequency peak disappears.

Pressure does not significantly influence the 100 kHz wave in WOMBAT. Instead, increasing pressure is observed to increase the level of the broadband structure in this frequency range. At higher pressures, the range over which the 100 kHz wave could be clearly discerned as a function of radial position is significantly reduced. Similarly at very low pressures (less than 0.8 mTorr) no clear peaks could be discerned in the 100 kHz range. The optimal pressure range for the 100 kHz wave is 0.8–1.2 mTorr with a clear maximum in signal to noise ratio (100 kHz relative to broadband structures) at 1 mTorr.

E. Power

The amplitude of the ion wave increases roughly in proportion to the power in the E.P. helicon source but there is no clear threshold. The wave is first unambiguously observed at $\sim$100 W. The maximum power of the generator (2 kW) did not allow for an investigation of an upper threshold. The frequency decreases slightly with increasing power.

For the wave to occur in WOMBAT, a lower limit for the input power is 1600 W, below which no clear peaks are observed. As power is increased above 1600 W (with1 mTorr and 110 G) the only significant observable effect is an increase in the 100 kHz signal amplitude and as a result an increase in the signal to noise ratio.

F. Magnetic field

Once again there is some evidence from the experiments in both systems that the frequency of the ion wave increases with magnetic field. In WOMBAT there is a minor increase as a function of magnetic field starting with 100 kHz at 100 G and reaching 123 kHz at 160 G and it appears that the frequency is proportional to the square root of the magnetic field; however, the data sample is small and the magnetic field changes a number of other parameters as well, so no real causal link can be established. Below 100 G the 100 kHz wave cannot be distinguished from the broadband structures. However above this limit, the peaks are clear and increase from 15 to 25 dB above the broadband noise floor for operating conditions when the pressure is set to 1 mTorr and forward power to 2.5 kW. As the magnetic field is increased to above 150 G, the signal to noise ratio decreases so that at 170 G the 100 kHz signal is only 5–10 dB above the noise floor. Unfortunately, the field strength cannot be increased beyond this limit and so it is not possible to deter-

mine whether there is also an upper limit to the magnetic field for which the 100 kHz wave is observable. Similar trends are observed in the E.P. system.

IV. DISCUSSION AND CONCLUSION

Ion acoustic wave phenomena have been observed in two helicon argon discharges—a small helicon source which is typically used as a plasma processing tool and a large magneto plasma device, WOMBAT. Though the E.P. helicon source is similar in conception to WOMBAT, there were a number of differences, notably chamber geometry, rf source frequency, antenna geometry, and magnetic field setup.

Nevertheless, there are a number of clear similarities between the two experiments: the low-frequency ion waves have a broadband frequency extending to about 1 MHz. Under certain conditions, narrow peaks of the order of 100–300 kHz are observed. All the low-frequency waves have a maximum amplitude at a radius which coincides with gradients in the plasma pressure. No low-frequency waves were found in the center of the discharge in either experiment, which was not the case in the earlier helicon experiments.[8–10] There were sidebands observed on either side of the helicon source frequency separated by the low ion wave frequency. The amplitude of these sidebands had a similar radial variation to the ion wave and did not follow the amplitude of the helicon wave. The experimental results suggest that the pump frequency of the helicon source, the plasma density and the volume of the plasma play little or no role in the observed behavior of the waves.

The magnetic field had a weak impact on the frequency of the ion wave that was observed to vary only as the square root in WOMBAT. A similar variation was observed in the E.P. machine as the pressure was varied. Without further investigation, it is not possible to draw any strong conclusions about this dependence as the form of the plasma itself changes with variations in the magnetic field and pressure.

In both systems the wave spectra could be considered characteristic of a parametric decay instability where a resonant interaction between three waves can result in a parametric decay process, which satisfies the conditions of energy conservation and momentum conservation. Energy conservation requires that the energy of the wave entering the interaction matrix is conserved and equal to the sum of the energy of all waves exiting the matrix, i.e., $\omega_0 = \omega_1 \pm \omega_2$ or more simply, the frequencies must add up. In both experiments presented here, the sum of the lower frequency helicon daughter and the low-frequency ion wave add up to the frequency of the helicon pump.

The momentum conservation equation can simply be written as $k_0 = k_1 + k_2$. Taking the energy and momentum conservation equations together, a simple rule appears that the group velocity of the pump and daughter should equal the phase velocity of the low-frequency ion wave. If the pump and daughter waves were electromagnetic helicons, their wavelength would be at least 20 times that of the ion wave making a linear addition of the wave vectors difficult. Even if we move into two dimensions, it is clearly not possible to arrange two small wave vectors to make a long wave vector. Hence, it would appear that the primary decay mechanism is not that of an electromagnetic helicon decaying to another electromagnetic helicon and an ion sound wave. The experimental results tend to bear this out as the low-frequency and daughter waves are not observed in the regions where the helicon has a maximum amplitude.

Consequently, the options left are that the decay is from waves on the resonance cone as suggested earlier[7] or that the ion waves are generated by the free energy in the radial plasma pressure gradient resulting from the electron temperature and density gradients. The resulting modulation in the refractive index at the ion wave frequency would cause the helicon wave to be modulated producing upper and lower sidebands that would, at least in the frequency domain, mimic a parametric decay.

In considering the possibility of a parametric decay, once again we would need to consider electrostatic waves and waves on the resonance cone and for the present experiments and for most helicon experiments, the pump frequency is sufficiently separated from the electron cyclotron frequency that the group velocity resonance cone angle is only a few degrees. In the E.P. system, the helicon wave generator frequency of 13.56 MHz and an electron gyro frequency of 84 MHz results in a resonance cone angle of $\sin^{-1}(0.16) = 9°$. Since there is 22 cm between the antenna and the median plane of the diffusion chamber (where measurements were made), one would expect the resonance cone to be at 3.7 cm from the projection of the antenna position (which corresponds to the gray line in Fig. 6) in this plane. There is a suggestion in Fig. 6(a) of a small minimum in the wave amplitude at this position but there is clearly no major maximum. For the ANU conditions, the resonance cone angle would be 1° or 2° so it would be difficult to say if the interaction were a parametric decay occurring close to the helicon antenna or a low-frequency instability generated by the radial pressure gradient which subsequently modulates the 7.2 MHz pump wave producing the upper and lower sidebands.

The ion wave clearly occurs at the edge of the plasma column for both experiments reported here, where there is a significant gradient in the plasma pressure. It is difficult, therefore, to be absolutely sure about the basic physics driving the ion waves which are observed. An electromagnetic parametric decay can be clearly ruled out but we cannot clearly differentiate between a parametric decay occuring on the resonance cone, a parametric decay occuring in the near fields of the antenna and propagating along the magnetic field lines that pass through the antenna or an instability driven by the radial pressure gradients modulating the helicon wave.

[1] R. W. Boswell, Plasma Phys. Controlled Fusion **26**, 1147 (1984).
[2] P. Chabert, J. Vac. Sci. Technol. B **19**, 1339 (2001).
[3] A. J. Perry, D. Vender, and R. W. Boswell, J. Vac. Sci. Technol. B **9**, 310 (1991).
[4] G. R. Tynan, A. D. Bailey III, G. A. Campbell *et al.*, J. Vac. Sci. Technol. A **15**, 2885 (1997).
[5] P. Zhu and R. W. Boswell, Phys. Rev. Lett. **63**, 2805 (1989).
[6] M. Porkolab, V. Aranasalam, and R. A. Ellis, Phys. Rev. Lett. **29**, 1438 (1972).
[7] R. W. Boswell and M. J. Giles, Phys. Rev. Lett. **36**, 1142 (1975).

[8]J. L. Kline, E. E. Scime, R. F. Boivin, A. M. Keesee, X. Sun, and V. S. Mikhailenko, Phys. Rev. Lett. **88**, 195002 (2002).
[9]J. L. Kline and E. E. Scime, Phys. Plasmas **10**, 135 (2003).
[10]V. F. Virko, G. S. Kirichenko, and K. P. Shamrai, Plasma Sources Sci. Technol. **12**, 217 (2003).
[11]M. Light, F. F. Chen, and P. L. Colestock, Phys. Plasmas **8**, 4675 (2001).
[12]R. W. Boswell, Phys. Lett. **33A**, 457 (1970).
[13]A. Cantin and R. R. J. Gagne, Appl. Phys. Lett. **30**, 31 (1977).
[14]M. B. Hopkins and W. G. Graham, Rev. Sci. Instrum. **57**, 2210 (1986).
[15]R. W. Boswell and R. K. Porteous, Appl. Phys. Lett. **50**, 1130 (1987).